

Low-Complexity Calibration of Mutually Coupled Non-Reciprocal Multi-Antenna OFDM Transceivers

Mark Petermann*, Markus Stefer#, Dirk Wübben*, Martin Schneider#, Karl-Dirk Kammeyer*

**Department of Communications Engineering*
University of Bremen, 28359 Bremen, Germany
 {petermann, wuebben, kammeyer}@ant.uni-bremen.de

#*RF & Microwave Engineering Laboratory*
University of Bremen, 28359 Bremen, Germany
 {markus.stefer, martin.schneider}@hf.uni-bremen.de

Abstract—In adaptive time division duplex (TDD) broadcast multi-antenna orthogonal frequency division multiplexing (OFDM) systems, non-reciprocal transceiver chains at the base station (BS) cause multi-user interference. This is due to the inappropriate spatial filter design at the BS based on the reverse link estimate. Hence, BS transceiver calibration is required. Provided that an estimate of the forward link channel is available at the BS, e.g., in a calibration phase, the transceiver parameters can be estimated by solving a total least squares (TLS) problem. In addition, if mutual coupling between the antennas exists the number of unknown front-end parameters to be estimated increases. Consequently, large matrices need to be decomposed via singular value decomposition (SVD) to attain a calibrated system. To deal with these large matrices a conjugate gradient (CG) method for solving the TLS problem iteratively is proposed in this paper. Simulation results show that the calibration based on the CG method achieves almost the same performance compared to the TLS solution but with significantly reduced complexity.

I. INTRODUCTION

The application of orthogonal frequency division multiplexing (OFDM) has become a state-of-the-art air interface technology for modern wireless communication systems [1]. In combination with multi-antenna arrays at the base station (BS) these systems are able to provide space division multiple access (SDMA) to multiple users (MU). With channel state information (CSI) at the BS based on uplink channel estimates in time division duplex (TDD) mode, adaptive schemes like frequency-domain pre-equalization can be applied [2]. A prerequisite for using the uplink estimates is channel reciprocity with respect to the baseband, which in general is not fulfilled as the uplink transmit-receive chain (Tx-Rx chain) is not reciprocal to the downlink (DL) Tx-Rx chain. Therefore, either robust pre-equalization schemes [2] or a suitable transceiver calibration is necessary [3].

It has been shown by the authors in [4] that robust filter design schemes for pre-equalization are insufficient for severe non-reciprocal conditions. Instead, the application of a relative calibration scheme based on a total least squares (TLS) formulation of the calibration problem (without coupling considerations) showed excellent properties in recovering almost

equivalent effective up- and downlink channels. The solution of the TLS problem is usually found via a singular value decomposition (SVD) [5]. If mutual coupling is present at the BS, the TLS problem formulation leads to large matrices, which need to be decomposed via SVD [3]. To overcome this problem, less complex algorithms must be used to find the solution of the equivalent minimum eigenvalue problem, e.g., by an inverse iterative power method [6]. In this contribution a low-complexity algorithm based on a conjugate gradient (CG) method for solving the TLS calibration problem in MU-Multiple Input Single Output (MISO)-OFDM systems is proposed. In this context, the BS not only has non-reciprocal transceivers but also is influenced by mutual coupling due to the narrow antenna element spacing of the array, e.g., in a femtocell BS.

The remainder of the paper is organized as follows. In Sec. II the system and the applied extended channel model are described. In addition, the non-reciprocity and the mutual coupling models are introduced. Subsequently, the downlink calibration schemes are stated in Sec. III. The relative calibration approach based on the SVD solution is reflected in Sec. III-A, while the CG method and complexity considerations are given in Sec. III-B and Sec. III-C, respectively. Simulation results for the calibration principles in different transceiver mismatch conditions are shown in Sec. IV. Finally, a conclusion is given in Sec. V.

II. SYSTEM MODEL

A. Extended Channel Model

A downlink (DL) scenario of a system with N_B base station antennas and N_M decentralized single-antenna mobile stations (MS) using OFDM with N_C subcarriers is considered, where $N_B \geq N_M$ should hold. The effective downlink matrix $\mathbf{H}(k)$ and the effective uplink (UL) matrix $\mathbf{G}(k)$ in frequency-domain on subcarrier k using a scattering matrix approach [2] can be written as

$$\mathbf{H}(k) = \mathbf{A}_{RM} \mathbf{W}_{RM} \mathbf{S}_{MB}(k) \mathbf{W}_{TB} \mathbf{A}_{TB}, \quad (1)$$

and

$$\mathbf{G}(k) = \mathbf{A}_{TM} \mathbf{W}_{TM}^T \mathbf{S}_{MB}(k) \mathbf{W}_{RB}^T \mathbf{A}_{RB}, \quad (2)$$

This work was supported in part by the German Research Foundation (DFG) under grant KA841/21-1 and SCHN1147/2-1.

respectively [4], [7]. Here, the indices T and R denote the transmit or receive chain at location M for the MS or B for the BS. The scattering matrix $\mathbf{S}_{MB}(k)$ can directly be replaced by the real physical downlink MIMO channel matrix $\mathbf{H}_{FD}(k)$ in frequency-domain [7]. The channel matrix $\mathbf{H}_{FD}(k)$ results from the frequency-selective time-domain channel matrix $\mathbf{H}_{TD}(\ell) \in \mathbb{C}^{N_M \times N_B}$, $0 \leq \ell \leq L_F - 1$, whose elements are i.i.d. complex Gaussian distributed. L_F denotes the number of uncorrelated channel taps.

Furthermore, in (1) and (2) the matrices

$$\mathbf{W}_{T[B/M]} = (\mathbf{I}_{N_{[B/M]}} - \mathbf{\Gamma}_{T[B/M]} \mathbf{S}_{[BB/MM]})^{-1} \quad (3a)$$

$$\mathbf{W}_{R[B/M]} = (\mathbf{I}_{N_{[B/M]}} - \mathbf{S}_{[BB/MM]} \mathbf{\Gamma}_{R[B/M]})^{-1} \quad (3b)$$

describe the mutual coupling and the reflection at the transceivers, whereas the matrices $\mathbf{A}_{[T/R][M/B]}$ contain the antenna gains in the transmit and the receive paths, respectively. If feedback effects of the BS antennas on the radiation of the MS is negligible, the matrices

$$\mathbf{A}_{[T/R]B} = \text{diag}\{\alpha_{[T/R]B,1}, \dots, \alpha_{[T/R]B,N_B}\} \quad (4a)$$

and

$$\mathbf{\Gamma}_{[T/R]B} = \text{diag}\{\gamma_{[T/R]B,1}, \dots, \gamma_{[T/R]B,N_B}\} \quad (4b)$$

with complex gain factors $\alpha_{[T/R],[B/M],[i/j]}$ and input/output reflection coefficients $\gamma_{[T/R],[B/M],[i,j]}$ can be modeled as diagonal matrices [7]. The modeling of these coefficients and a detailed description of the scattering matrices $\mathbf{S}_{[BB/MM]}$ are given separately in Sec. II-B. Without loss of generality, frequency-flat characteristics of the transceiver chains is assumed throughout the paper, meaning that the matrices \mathbf{A} and \mathbf{W} are independent of subcarrier index k (cf. (1) and (2)).

If linear pre-equalization is applied in the considered multi-user broadcast MISO-OFDM system the receive signal $\mathbf{y}(k) = [y_1(k), \dots, y_{N_M}(k)]^T$ on subcarrier k stacking all mobile stations reads

$$\mathbf{y}(k) = \beta(k) \mathbf{H}(k) \mathbf{F}(k) \mathbf{d}(k) + \mathbf{n}(k), \quad (5)$$

where $\mathbf{d}(k) \in \mathbb{C}^{N_M \times 1}$ is the data vector to be transmitted to the N_M MS. The pre-equalization matrix $\mathbf{F}(k) \in \mathbb{C}^{N_B \times N_M}$ in the minimum mean square error (MMSE) case is determined using the uplink channel matrix $\mathbf{G}(k)$ such that

$$\mathbf{F}_{\text{MMSE}}(k) = \mathbf{G}^H(k) (\mathbf{G}(k) \mathbf{G}^H(k) + \sigma_n^2 \mathbf{I}_{N_M})^{-1} \quad (6)$$

holds. Here, the same noise power σ_n^2 on all subcarriers and all MS is assumed. The scalar $\beta(k)$ is chosen such that the total sum power constraint per subcarrier is fulfilled [4].

In terms of MMSE channel estimation in uplink direction, the estimated channel matrix $\hat{\mathbf{G}}(k)$ of one subcarrier can be modeled by [8]

$$\hat{\mathbf{G}}(k) = \sqrt{1 - \sigma_e^2} \mathbf{G}(k) + \sqrt{\sigma_e^2 (1 - \sigma_e^2)} \mathbf{\Psi}(k), \quad (7)$$

where $\mathbf{\Psi}(k)$ a Gaussian error matrix with an entry variance of one and σ_e^2 is the estimation error variance. The same holds for $\hat{\mathbf{H}}(k)$ with an independent error matrix but here with identical estimation error variance, which generally does not need to be the same.

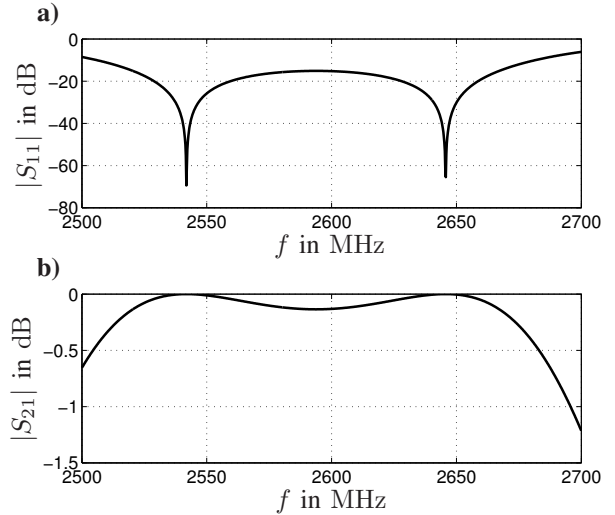


Fig. 1. Scattering parameters of an exemplary bandpass filter at $f_c = 2.6$ GHz

a) Input reflection coefficient S_{11} - b) Transfer factor S_{21}

B. Mutual Coupling and Error Models

Concerning the error model of the complex gain factors that describe the non-reciprocal behavior of the transceiver chains each gain factor $\alpha_{[T/R]B,i}$ in (4a) is assumed to be slightly mismatched. Consequently, $\alpha_{[T/R]B,i} = 1 + \delta_{[T/R]B,i}$ holds, where the statistically independent error terms $\delta_{[T/R]B,i}$ are zero mean complex Gaussian random variables with variance σ_δ^2 [2]. These factors are expected to change very slowly in time compared to the duplex phase and are assumed to be equal per antenna on all subcarriers k .

The modeling of the reflection coefficients $\gamma_{[T/R]B,i}$ is motivated by an exemplary filter for a long-term evolution (LTE) band at 2.6 GHz. The scattering parameters of this filter are shown in Fig. 1a) and b). Since the input reflection coefficient S_{11} is around 20 dB below the transmission factor S_{21} in the frequency range of interest, the mean value for $\gamma_{[T/R]B,i}$ is set to 0.1. Then

$$\gamma_{[T/R]B,i} = 0.1 + \kappa_{[T/R]B,i} \quad (8)$$

is used to model the reflection coefficient in (4b). Again additional error terms $\kappa_{[T/R]B,i}$ are added, which are zero mean complex Gaussian random variables with variance σ_κ^2 .

To determine the scattering matrices $\mathbf{S}_{[BB/MM]}$ in (3), the antenna array configurations need to be investigated from an electromagnetic perspective. If at least two antennas are in proximity regarding the wavelength λ and one of these antennas is transmitting, the second is irretrievably in the near-field of the transmitting antenna. As a result, the transmitting antenna induces a voltage at the ports of the second antenna, which is not transmitting. This induced voltage can be related to the impressed current on the transmitting antenna, which gives the mutual impedance. Hence, the mutual impedance is a measure for the strength of the antenna coupling due to the near-field interaction. Taking also the input impedance Z_A of a single antenna element into account, the following relation between the antenna currents I_i and voltages V_i can

be established at the BS

$$V_i = Z_A \cdot I_i + \sum_{j=1, j \neq i}^{N_B} Z_{ij} \cdot I_j, \quad (9)$$

with Z_{ij} denoting the mutual impedance between the antenna elements i and j [9]. Here, "infinitesimally thin" $\lambda/2$ dipoles are considered for the antenna elements [10]. The input as well as the mutual impedance can be computed by using the results presented in [11]. Rewriting the current and voltage relations indicated by (9) in matrix form, the impedance matrix $\mathbf{Z} \in \mathbb{C}^{N_B \times N_B}$ is obtained. The latter can be used to describe the scattering parameter matrix \mathbf{S}_{BB} of the base station antenna array exploiting the following relation [12]

$$\mathbf{S}_{BB} = \left(\frac{\mathbf{Z}}{Z_0} + \mathbf{I}_{N_B} \right)^{-1} \left(\frac{\mathbf{Z}}{Z_0} - \mathbf{I}_{N_B} \right). \quad (10)$$

Here, $Z_0 = 50 \Omega$ denotes the characteristic impedance of the ports.

It is assumed that no coupling is present between the MS as the spacing between the users is at least of several wavelengths such that $\mathbf{S}_{MM} = \frac{Z_A}{Z_0} \mathbf{I}_M$, $\gamma_{[T/R]M,j} \approx 0$ and hence $\mathbf{W}_{[T/R]M} \approx \mathbf{I}_M$. In addition, the gain factors in matrices $\mathbf{A}_{[T/R]M}$ can be set to one as they have no impact on the system performance [2]. Using the model for $\alpha_{[T/R]B,i}$ as well as (8) and (10), the matrices \mathbf{W}_{TB} and \mathbf{W}_{RB} in (3) can be calculated.

III. DOWNLINK CHANNEL CALIBRATION

A. Calibration via Singular Value Decomposition (SVD)

For the following derivations of the calibration approach it is assumed that both the estimated CSI of the uplink and downlink channel are known at the BS. This can be achieved in a special calibration phase or by means of analog feedback of the DL channel. Hence, errors in all variables are obtained due to the estimation, where we neglect the $\hat{\cdot}$ -indication for the remainder of this section.

Starting with (2) and resolving it with respect to \mathbf{S}_{MB} , inserting the result into (1) leads to

$$\mathbf{H}(k) = \underbrace{\mathbf{A}_{RM} \mathbf{W}_{RM} \mathbf{W}_{TM}^{-T} \mathbf{A}_{TM}^{-1}}_{\mathbf{C}_M} \mathbf{G}(k) \underbrace{\mathbf{A}_{RB}^{-1} \mathbf{W}_{RB}^{-T} \mathbf{W}_{TB} \mathbf{A}_{TB}}_{\mathbf{C}_B}. \quad (11)$$

We define the auxiliary vectors $\mathbf{c}_B \triangleq \text{vec}\{\mathbf{C}_B^{-1}\}$ and $\mathbf{c}_M \triangleq \text{vec}\{\mathbf{C}_M^T\}$, where the vec-operator is defined as $\text{vec}\{\mathbf{B}\} = \text{vec}\{[\mathbf{b}_1 \dots \mathbf{b}_i]\} = [\mathbf{b}_1^T, \dots, \mathbf{b}_i^T]^T$, and $\mathbf{g}_i(k)$ is the i -th column of matrix $\mathbf{G}(k)$. Then, (11) can be reformulated with

$$\Theta(k) = \begin{bmatrix} \mathbf{I}_{N_M} \otimes \mathbf{g}_1^T(k) \\ \vdots \\ \mathbf{I}_{N_M} \otimes \mathbf{g}_{N_B}^T(k) \end{bmatrix} \text{ and } \Omega(k) = \mathbf{I}_{N_B} \otimes \mathbf{H}(k) \quad (12)$$

to

$$\Omega(k) \mathbf{c}_B - \Theta(k) \mathbf{c}_M = \mathbf{0}_{N_B N_M \times 1}, \quad (13)$$

where \otimes is the Kronecker product. Set $\mathbf{c} \triangleq [\mathbf{c}_B^T \ \mathbf{c}_M^T]^T$ as well as

$$\mathbf{E}_k = [\Omega(k) \quad -\Theta(k)] \quad (14a)$$

and

$$\mathbf{E} = [\mathbf{E}_1^T, \dots, \mathbf{E}_K^T]^T \in \mathbb{C}^{K N_B N_M \times N_B^2 + N_M^2}. \quad (14b)$$

Thus, (13) can be rewritten to

$$\mathbf{E} \mathbf{c} = \mathbf{0}_{K N_B N_M \times 1}. \quad (15)$$

Obviously \mathbf{E} depends on $\mathbf{G}(k)$ and $\mathbf{H}(k)$ (cf. [3]). Here, K defines the number of subcarriers used for calibration, where the k 's can be arbitrarily chosen due to the presumed frequency-flat characteristics of the transceivers. As there are $N_M^2 + N_B^2$ number of unknowns and $K \cdot N_M N_B$ linear equations, multiple subcarriers K are necessary to solve (15).

As described in [3], (15) defines a special case of a total least squares (TLS) problem [5], where the optimization problem is defined as

$$\underset{\Delta \mathbf{E}}{\text{minimize}} \quad \|\Delta \mathbf{E}\|_F \quad (16a)$$

$$\text{such that} \quad (\mathbf{E} + \Delta \mathbf{E}) \mathbf{c} = \mathbf{0}_{K \cdot N_B N_M \times 1}. \quad (16b)$$

The goal is to find a perturbation matrix $\Delta \mathbf{E}$ with minimum Frobenius norm that lowers the rank of \mathbf{E} , where $\Delta \mathbf{E}$ is the correction term of the TLS optimization problem.

The solution to (15) lies in the right null space of \mathbf{E} and can be computed with the singular value decomposition (SVD). In [5] the connection of the TLS solution to the SVD was shown. Then, if $\mathbf{E} = \mathbf{U} \Sigma \mathbf{V}^H$ depicts the SVD and matrix $\mathbf{V} = [\mathbf{v}_1, \dots, \mathbf{v}_{N_B + N_M}]$ denotes the right singular vector space, the estimated solution for \mathbf{c} depends on the right singular vector corresponding to the smallest singular value in Σ such that $\mathbf{c}_{\text{TLS}} = -\frac{1}{v_{N_B + N_M, N_B + N_M}} \mathbf{v}_{N_B + N_M}$. Thus, \mathbf{c} can be fully determined (up to a scalar coefficient, which vanishes due to the reciprocal multiplication in (11)) if and only if $v_{N_B + N_M, N_B + N_M} \neq 0$ holds [5]. Finally, with solution vector \mathbf{c}_{TLS} the matrices $\mathbf{G}(k)$ can be adjusted according to (11).

B. Conjugate Gradient Method for Solving the TLS Problem

The problem of the SVD-based TLS algorithm is that it can be computationally prohibitive for large matrices \mathbf{E} . It was shown that the constrained minimization problem in (16) is equivalent to minimizing the so-called Rayleigh quotient [13]

$$f(\mathbf{c}) = \frac{\mathbf{c}^H \mathbf{E}^H \mathbf{E} \mathbf{c}}{\mathbf{c}^H \mathbf{c}}. \quad (17)$$

The minimization of the Rayleigh quotient in turn is equivalent in finding the eigenvector \mathbf{c} associated with the smallest eigenvalue of matrix $\mathbf{E}^H \mathbf{E}$ such that $\min\{\|\Delta \mathbf{E}\|_F^2\} = \min\{f(\mathbf{c})\}$ equals the minimum singular value and the TLS solution is obtained [14]. An advantage of the Rayleigh quotient is the fact that (17) can be minimized iteratively. One possibility is to use an inverse power method to find the corresponding eigenvector [6]. Applying the Rayleigh quotient introduces a shift equal to this quotient into the inverse iteration [13]. To

avoid a matrix inverse, this can be solved via a conjugate gradient (CG) method, e.g., according to [14].

The CG method successively approximates the vector \mathbf{c} in iteration m such that

$$\mathbf{c}_{m+1} = \mathbf{c}_m + \xi_m \mathbf{s}_m, \quad (18)$$

where \mathbf{s}_m is the search direction and ξ_m the step size. Following [15], after taking the derivative of (17) and minimizing it, the step size is the solution of a quadratic equation and is always real, where the smaller value of the two possible solutions corresponds to the minimum eigenvalue such that [14]

$$\xi_m = \frac{\sqrt{b^2 - 4 \cdot d \cdot c} - b}{2 \cdot d}, \quad (19)$$

with the definitions of b, c and d as in Alg. 1. Now, to update the solution vector \mathbf{c}_{m+1} iteratively, the calculations listed in **Algorithm 1** are executed. The algorithm either stops after m_{\max} iterations or if the change of the estimated smallest singular value falls below a certain threshold, which is set to $\epsilon_{\text{thres}} = 10^{-5}$ here.

Algorithm 1 CG Minimization of Rayleigh Quotient

Require: $\Phi = \mathbf{E}^H \mathbf{E}$

- 1: $\mathbf{c}_0 = [\mathbf{0}_{N_B^2 + N_M^2 - 1}, 1]^T$ {initial guess}
- 2: $\rho_0 = \mathbf{c}_0^H \Phi \mathbf{c}_0$ {estimated smallest eigenvalue}
- 3: $\mathbf{r}_0 = \rho \mathbf{c}_0 - \Phi \mathbf{c}_0$ {residual}
- 4: $\mathbf{s}_0 = \mathbf{r}_0$ and $m = 0$ and $\epsilon = -\infty$ {initialize variables}
- 5: **while** $|\epsilon| > \epsilon_{\text{thres}}$ and $m < m_{\max}$ **do**
- 6: $\Upsilon_{a,m} = \mathbf{c}_m^H \Phi \mathbf{s}_m$ and $\Upsilon_{b,m} = \mathbf{s}_m^H \Phi \mathbf{s}_m$
- 7: $\Upsilon_{c,m} = \mathbf{s}_m^H \mathbf{c}_m$ and $\Upsilon_{d,m} = \mathbf{s}_m^H \mathbf{s}_m$
- 8: $b = \Upsilon_{b,m} - \rho_m \Upsilon_{d,m}$ and $c = \Upsilon_{a,m} - \rho_m \Upsilon_{c,m}$
- 9: $d = \Upsilon_{b,m} \Upsilon_{c,m} - \Upsilon_{a,m} \Upsilon_{d,m}$
- 10: $\xi_m = \frac{\sqrt{b^2 - 4dc} - b}{2d}$
- 11: $\mathbf{c}_{m+1} = \mathbf{c}_m + \xi_m \mathbf{s}_m$ {update eigenvector}
- 12: $\mathbf{c}_{m+1} = \frac{\mathbf{c}_{m+1}}{\|\mathbf{c}_{m+1}\|_2}$
- 13: $\rho_{m+1} = \mathbf{c}_{m+1}^H \Phi \mathbf{c}_{m+1}$ {update Rayleigh quotient}
- 14: $\mathbf{r}_{m+1} = \rho_{m+1} \mathbf{c}_{m+1} - \Phi \mathbf{c}_{m+1}$
- 15: $\psi_m = -\frac{\mathbf{s}_m^H \Phi \mathbf{r}_{m+1}}{\mathbf{s}_m^H \Phi \mathbf{s}_m}$
- 16: $\mathbf{s}_{m+1} = \mathbf{r}_{m+1} + \psi_m \mathbf{s}_m$ {update search direction}
- 17: $\epsilon = \frac{\rho_{m+1} - \rho_m}{\rho_m}$ {check convergence}
- 18: **if** $\epsilon > 0$ **then**
- 19: $\mathbf{c}_{m+1} = \mathbf{c}_m$ {correct wrong gradient search}
- 20: **break** {stop algorithm earlier}
- 21: **end if**
- 22: $m \leftarrow m + 1$
- 23: **end while**
- 24: **return** $\mathbf{c}_{\text{CG}} = -\frac{\mathbf{c}_{m-1}}{\mathbf{c}_{N_B + N_M}^2}$ {approx. TLS solution}

C. Complexity Considerations

The complexity of the SVD depends on the number of parameters to be estimated, meaning the length of vector $\mathbf{c} \in \mathbb{C}^{N_M^2 + N_B^2 \times 1}$. In general, the common SVD calculation needs around $\mathcal{O}\left(\left(N_M^2 + N_B^2\right)^3\right)$ multiplications, which is not suitable for large scale matrices \mathbf{E} . Following [14], the complexity of the CG method is in the order of $\mathcal{O}\left(\left(N_M^2 + N_B^2\right)^2\right)$

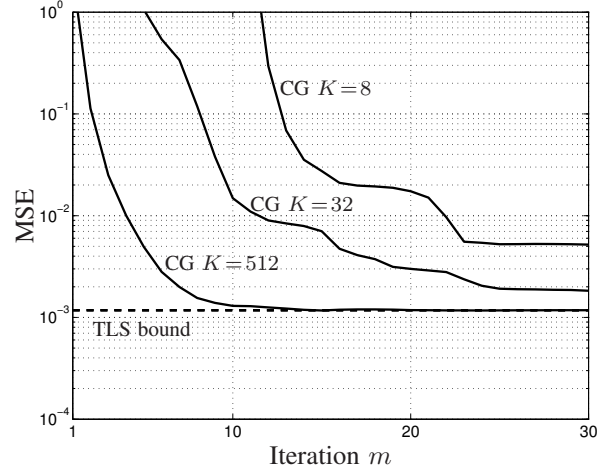


Fig. 2. Exemplary convergence behavior of the conjugate gradient method for a MU-MISO-OFDM system with $N_C = 512$ subcarriers and different numbers of K

per iteration. In addition, it is well known that the CG method converges quite fast. In Fig. 2 an exemplary convergence behavior of the CG method for $N_C = 512$, $\sigma_e^2 = 10^{-4}$ and different numbers of calibration carriers K is shown. The mean square error (MSE) describes the remaining error between the true effective DL channel and the estimated channel after calibration. Increasing K proves to be accurate and additionally converges faster to the TLS solution compared to smaller K . Hence, for large K , and consequently large matrices \mathbf{E} , the CG method is explicitly suitable for the calibration process.

IV. SIMULATION RESULTS

In this section, bit error rate results versus E_b/N_0 for linear MMSE pre-equalization in a $N_B = N_M = 4$ multi-user MISO-OFDM scenario applying $N_C = 256$ subcarriers and 16-QAM transmission are shown. The utilized QAM soft output demapping is done via max-log approximation. The E_b/N_0 -ratio is defined as $E_b/N_0 = 1/(R_c \log_2(M) \sigma_n^2)$, where R_c is the code rate of the applied channel code. The applied channel code in the encoded scenarios is a half-rate punctured 3GPP Turbo Code with additional sub-block interleaving [1]. It is assumed that a codeword ranges over six OFDM symbols. The guard interval has a length of $N_g = 6$, which is set equal to the length of the considered Rayleigh channel taps at symbol clock L_F . The channel has an almost exponentially decaying power delay profile. Furthermore, the channel is assumed to be constant for one codeword but changes from codeword to codeword and the channel estimation error is $\sigma_e^2 = 10^{-4}$. For completeness, it has to be mentioned that the guard loss is also considered in the results. The variance of the reflection coefficients at the BS is fixed to $\sigma_\kappa^2 = -30$ dB for all simulations.

Fig. 3 shows the results, where subfigures **a)** for $\sigma_\delta^2 = -30$ dB and **b)** for $\sigma_\delta^2 = -20$ dB present the uncoded results and **c)** ($\sigma_\delta^2 = -20$ dB) and **d)** ($\sigma_\delta^2 = -10$ dB) the coded results, respectively. The uncoded results show a significantly decreased performance if no calibration is applied. The calibration results for $K = 32$ indicate that only with a

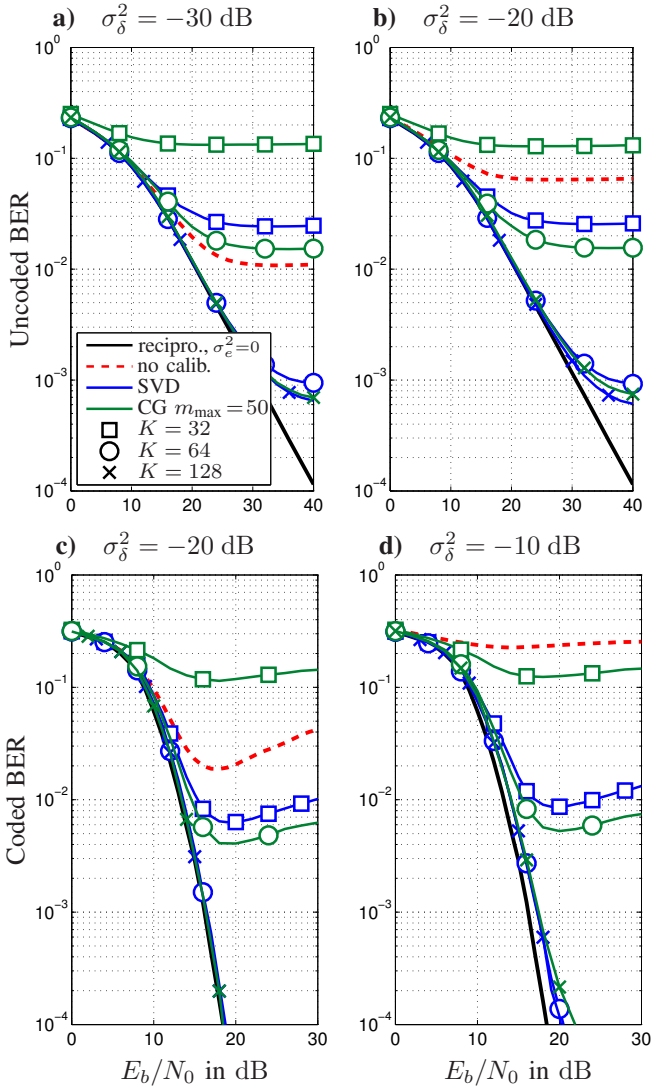


Fig. 3. BER versus E_b/N_0 for a system with $N_B = N_M = 4$ and BS antenna coupling ($\sigma_\kappa^2 = -30$ dB), $N_C = 256$ subcarriers and 16-QAM with MMSE pre-equalization and different calibration schemes. The channel estimation error variance is $\sigma_e^2 = 10^{-4}$ and the applied channel code in **c**) and **d**) is a half-rate punctured turbo code.

large number of calibration carriers sufficient linear equations are available to ensure a good estimate of vector \mathbf{c} . Otherwise a decrease in BER is apparent. While the SVD solution achieves a good performance for $K = 64$ in the uncoded case, the CG method with $m_{\max} = 50$ needs more carriers to significantly improve the average BER of the users. In case of $K = 128$ the CG method has the same performance gain compared to the direct SVD but with considerably reduced complexity. This substantiates the fact that the CG method is especially applicable for large-scale matrix problems [13]. With the utilization of channel coding the system itself is more robust to reciprocity mismatch. Nevertheless, calibration is necessary as non-reciprocal transceiver lead to an error floor. The increasing error rates are in accordance to the results in [4]. Utilizing the calibration employing $K = 128$ carriers leads almost to the same performance as for the reciprocal system with perfect channel estimation. Again, the CG method performs slightly

worse with less carriers but works as good as the direct SVD for $K \rightarrow N_C$ in the region of interest around a BER of 10^{-3} .

Remark: To ensure an average low BER in coded scenarios, cases of divergence must be avoided. Because a strong channel code guarantees minor occurrences at high SNRs, the calibration results can be allowed to be less accurate. Therefore, ϵ_{thres} should be chosen larger or the lines 18 to 21 in Alg. 1 can be used to avoid a wrong direction of the gradient. In contrast, without channel coding a case of divergence does not significantly contribute to the error rates.

V. CONCLUSION

In this paper, it has been shown that relative calibration techniques for mutually coupled MU-MISO-OFDM systems with decentralized receivers are able to combat the non-reciprocal transceiver chains in terms of DL BER if estimated instantaneous UL/DL-CSI is available at the BS. The CG method is an iterative low-complexity solution to approximate the ordinary TLS solution based on direct SVD. Increasing the number of subcarriers in the TLS approach proved to show better performance in these systems. The increasing complexity is manageable by applying a CG algorithm, which in addition has faster convergence with more calibration carriers.

REFERENCES

- [1] 3GPP TSG RAN, "E-UTRA; Multiplexing and Channel Coding (Release 8)," 3GPP, Tech. Rep. 36.212 V8.7.0, May 2009.
- [2] R. Habendorf and G. Fettweis, "Pre-Equalization for TDD Systems with Imperfect Transceiver Calibration," in *IEEE Proc. Vehicular Technology Conference (VTC), Spring*, Marina Bay, Singapore, May 2008.
- [3] M. Guillaud, "Transmission and Channel Modeling Techniques for Multiple-Antenna Communication Systems," PhD thesis, Ecole Nationale Supérieure des Telecommunications, Paris, France, Jul. 2005.
- [4] M. Petermann, D. Wübben, and K.-D. Kammeyer, "Evaluation of Encoded MU-MISO-OFDM Systems in TDD Mode with Non-ideal Channel Reciprocity," in *8th International ITG Conference on Source and Channel Coding (SCC 2010)*, Siegen, Germany, Jan. 2010.
- [5] G. H. Golub and C. F. V. Loan, "An Analysis of the Total Least Squares Problem," *SIAM Journal on Numerical Analysis*, vol. 17, no. 6, pp. 883–893, Dec. 1981.
- [6] —, *Matrix Computations*, 3rd ed. Johns Hopkins Univ. Press, 1996.
- [7] W. Keusgen, "Antennenkonfiguration und Kalibrierungskonzepte für die Realisierung reziproker Mehrantennensysteme," PhD thesis (in German), RWTH Aachen, Germany, Oct. 2005.
- [8] P. Xia, S. Zhou, and G. B. Giannakis, "Adaptive MIMO OFDM based on Partial Channel State Information," *IEEE Trans. Signal Process.*, vol. 52, no. 1, pp. 202–213, Jan. 2004.
- [9] T. Svantesson, "The Effects of Mutual Coupling Using a Linear Array of thin Dipoles of Finite Length," in *8th IEEE Signal Processing Workshop On Statistical Signal Processing*, Portland, USA, Sep 1998.
- [10] M. Stefer and M. Schneider, "On Modeling Antenna Coupling for Adaptive MIMO-OFDM Systems," in *International ITG Workshop on Smart Antennas (WSA 2010)*, Bremen, Germany, Feb. 2010.
- [11] S. A. Schelkunoff and H. T. Friis, *Antennas - Theory And Practice*, 3rd ed. John Wiley & Sons, 1966.
- [12] D. Pozar, *Microwave Engineering*, 2nd ed. John Wiley & Sons, 1998.
- [13] A. Björck, P. Heggernes, and P. Matstoms, "Methods for Large Scale Total Least Squares Problems," *SIAM. Journal on Matrix Anal. & Appl.*, vol. 22, no. 2, pp. 413–429, 2000.
- [14] W. Zhu, Y. Wang, Y. Yao, J. Chang, H. L. Graber, and R. L. Barbour, "Iterative Total Least-Squares Image Reconstruction Algorithm for Optical Tomography by the Conjugate Gradient Method," *Journal of Opt. Soc. of America*, vol. 14, no. 4, pp. 799–807, Apr. 1997.
- [15] I. Shavitt, C. F. Bender, A. Pipano, and R. P. Hosteny, "The Iterative Calculation of Several of the Lowest or Highest Eigenvalues and Corresponding Eigenvector of Very Large Symmetric Matrices," *Journal Comput. Phys.*, vol. 11, pp. 90–108, Nov. 1973.